Turbulent Motion and Mixing in a Pipe

JON LEE and ROBERT S. BRODKEY

The Ohio State University, Columbus, Ohio

Turbulent mixing of a dye solution injected at the center of a pipe was studied by means of a new light probe developed for the measurement of concentration fluctuations. The measurements of mean concentration and intensity of concentration fluctuations were made both along the axial distance and across the pipe. The concentration fluctuations persisted longer at the center-line region than anywhere else; this suggested the use of the decay of intensity at the center as an upper limit. Approximately 99% of the initial intensity decayed within 7.5 ft. (30 L/d). The concentration spectra along the axial distance indicated that the eddies initially undergo a scalar energy cascade. Because of the huge difference in the kinematic viscosity and molecular diffusivities the concentration spectra extend much farther toward high wave numbers than the velocity spectrum. Apparently a state of imbalance resulted between the supply of small eddies and their dissipation; this was marked by the appearance of a small hump in the spectra. The phenomenological approximations of Corrsin and of Beek and Miller could be used for the practical problem of predicting the decay of the intensity of the concentration fluctuations or mixing in the pipe geometry studied.

The principles of mixing on a macroscopic level have been known and used effectively for a number of years for the scale-up of mixing processes. However these scale-up methods have been somewhat empirical in nature owing to the lack of information about mixing theory on a microscopic level. The complexity of the problems involving turbulence has made a quantitative approach difficult. However the recent advances in the knowledge about statistical turbulent motion have opened up the field of mixing to potentially a new degree of understanding.

If the scalar quantity (heat or mass) is a stochastic variable, the mean value and the statistical functions for the deviation from the mean are important. This latter variable is the intensity {or root mean squared (r.m.s.) value} of the fluctuations. The intensity is a measure of amplitude and goes to zero when the mixing is completed (*9*). Actually the intensity must be measured over some small but finite volume. If this volume is too small, statistical fluctuations in the number of molecules present will be detected, and if it is too large, the measurement would become insensitive.

The turbulent mixing problem was developed in the same manner as turbulent motion theory by Obukhov (*19*) and Corrsin (*5, 6*). Corrsin (*7*) later suggested an exponential type of decay for the intensity of the scalar fluctuations (under a restricted turbulent field). In an attempt to describe the decay for the general case Beek and Miller (*2*) solved the equation for the scalar covariance, using Heisenberg's eddy-diffusivity type of approximation.

Corrsin and his co-workers (*11, 17*) have made a series of experiments for the study of the statistical structure of a scalar field; their works dealt with air flow in a wind tunnel, and extensive use of hot-wire anemometry was made for the measurement of temperature fluctuations. For the measurement of concentration fluctuations in a gas stream Rosensweig, Hottel, and Williams (*22*) have recently developed an optical technique based on light scattering, and reported results for the mixing of smoke into air. Prausnitz and Wilhelm (*20*) and Lamb, Manning, and Wilhelm (*12*) have developed an electrical conductivity probe which is sensitive to the conductivity of a salt solution; with this type of probe Prausnitz and Wilhelm (*21*) studied mixing in a liquid fluidized bed, and Manning and Wilhelm (*16*) studied mixing in a stirred tank under continuous flow conditions.

In this work the primary interest is the study of turbulent mixing of a secondary fluid injected at the center of a 3-in. pipe in which water flows turbulently. Many experiments of this type have been made (water or air) in order to measure either the mean scalar profile throughout the whole region of a pipe or some statistical quantities at the central part. The experiments to be described differ from the others in several aspects, one of which is that the mean concentration profile and intensity of concentration fluctuations throughout the whole pipe have been measured in a system where the velocity field is well known (*3, 13*). The spectra of velocity and concentration fluctuations have also been measured. An even more important difference in the present experiments was the use of dye as the scalar in a water system. This combination has an extremely small molecular diffusivity and thus should make the molecular mixing process an appreciable contributor to the total mixing time.

THEORY

As in the turbulent motion problem the formulation of the turbulent mixing problem in terms of various statistical moments gives rise to an infinite set of equations, the closure of which cannot be deduced entirely from the theory

Jon Lee is with the Wright-Patterson Air Force Base, Dayton, Ohio.

itself. A detailed discussion on the closure problem for the scalar equations can be found elsewhere (*14, 18*). The brief discussion to follow is restricted to the second-moment equation, since it is used in the interpretation of experimental results observed in turbulent mixing in a pipe.

For the equation for the scalar quantity intensity Corrsin writes (*5, 7*)

$$\frac{d\overline{s^2(t)}}{dt} = -12\,D\,\frac{\overline{s^2(t)}}{\lambda_s^2(t)} \tag{1}$$

where $\overline{s^2(t)}$ is the mean-squared scalar fluctuation and $\lambda_s(t)$ is the scalar microscale. Equation (1) has a very simple form; the solution of such first-order equations can be obtained readily by quadrature, provided the time dependence of $\lambda_s^2(t)$ is specified explicitly.

Corrsin (*7*) suggested a round about path to impose some restrictions on the turbulent field in order to justify the assumption that $\lambda_s^2(t)$ has a very weak time dependence. He has further suggested that for a low Schmidt number (ν/D)

$$\frac{\lambda_s^2}{\lambda_f^2} = \frac{D}{\nu} \quad \text{or} \quad \frac{\lambda_s^2}{\lambda_g^2} = \frac{D}{\nu} \tag{2}$$

With the use of Equation (2), Equation (1) can be integrated to give an exponential decay law

$$\overline{s^2(t)} = \overline{s^2(o)}\; e^{-t/\tau} \tag{3}$$

where τ is

$$\tau = \lambda_s^2/12\,D = \lambda_g^2/6\nu \tag{4}$$

Using a different approach Corrsin (*8*) has recently used the work of Batchelor (*1*) to extend these results to the high Schmidt number range. First, for the low Schmidt number case, the time constant of Equation (4) can be expressed as

$$\tau = \lambda_s^2/12\,D = (5/\pi)^{2/3}\,(L_s^2/\epsilon)^{1/3} \tag{5}$$

For the high Schmidt number case the time constant becomes

$$\tau = \lambda_s^2/12\,D = (1/2)\,[3\,(5/\pi)^{2/3}\,(L_s^2/\epsilon)^{1/3} + (\nu/\epsilon)^{1/2} \ln N_{Sc}] \tag{6}$$

This latter form removes a serious criticism (*14*) of the earlier work, that is the lack of a dependance on the Schmidt number. As can be seen from Equation (6) the requirement of no mixing in the limit of infinite Schmidt number is now satisfied [$\tau = \infty$, which gives $\overline{s^2(t)} = \overline{s^2(0)}$ for all time].

An alternate approach is to take the Fourier transform of the second-order moment equation into wave number space. Corrsin (*4*) has suggested using the transformed equation with the Heisenberg eddy-diffusivity type of transfer function for the scalar field. Thus the rate of transfer of scalar quantity energy through wave number k may be expressed as (*2*)

$$\frac{\partial}{\partial t}\int_o^k E_s(k,t)\,dk = -2[D + \epsilon_s(k,t)] \int_o^k k^2 E_s(k,t)\,dk \tag{7}$$

and

$$\epsilon_s(k,t) = \int_k^\infty \left(\frac{E(k,t)}{k^3}\right)^{1/2} dk \tag{8}$$

Since Equations (7) and (8) are analogous to Heisenberg's eddy-viscosity type of analysis, one can expect that it will contain not only the good points of Heisenberg's transfer function but also will be subject to criticisms such as put forward by Hinze (*10*). Recently Beek and Miller (*2*) integrated Equations (7) and (8) numerically for $E_s(k, t)$ and subsequently from this obtained the scalar intensity. A number of assumptions had to be introduced; for example they adopted a physical model of isotropic turbulence, which is fictitiously enclosed in a pipe and conveyed by a uniform mean velocity. Turbulent shear flow does provide such a stationary turbulent velocity field but is certainly not isotropic. Further criticism (*14*) about the boundary conditions for the scalar injection can be made. Nevertheless this is one of the few solutions to turbulent mixing available and thus should be considered further.

From the work of Beek and Miller the following comments can be made. The general shapes of the $E_s(k, t)$ curves are considerably different for low and high Schmidt numbers. For $\nu \cong D$ the various equilibrium subranges for $E_s(k,t)$ essentially overlap those for $E(k,t)$. Thus one might expect that $E_s(k, t)$ and $E(k, t)$ are similar in shape. On the other hand for $\nu >> D$, $E_s(k, t)$ extends far beyond the cutoff wave number for $E(k, t)$. The convective subrange of the scalar field overlaps the dissipation subrange of the velocity field, thus creating a state of imbalance between the convective and dissipative subranges for the scalar field. This was indicated by a hump in the higher wave number range for the scalar field; this hump seems to mark the separation between the two subranges. Another point is that the influence of turbulence in the velocity field (measured in terms of overall pipe Reynolds number) has a greater effect for the case of high than for low Schmidt numbers.

EXPERIMENTAL

The equipment involved in this experiment could be classified as the flow system which provided the proper turbulent velocity and concentration fields studied and the measuring systems which allowed probing the variations in the characteristic variables of interest.

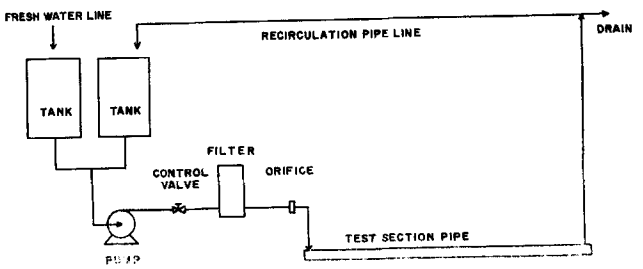

Fig. 1. Layout of flow system.

The flow system is shown in Figures 1 and 2. The filter was equipped with 5-μ filter elements. The test section was a straight, seamless, and jointless polyethylene pipe of 3.068 in. I.D. and about 48-ft. in length, which was considered sufficient to eliminate the undesirable entrance effects. For mixing measurements the secondary fluid or dye had to be introduced smoothly; consequently a constant head system was used. This gravity feed method had an advantage over the use of a pumping system, which would have some periodicity associated with it. This repetitive nature might be picked up in spectrum measurements and would complicate the interpretation of data. The secondary fluid was always injected at the center of the pipe, but it was desirable to allow an arbitrary distance between the points of injection and detection. Since the position of the detector remained stationary at 5-ft. from the downstream end of the test section, the long thin stainless steel tube (¼-in. diameter, 44 ft. long) was introduced from the upstream end. The injection end could be adjusted by inserting this tube to different lengths. It was positioned at the center of the test section pipe by means of a number of supports

which consisted of three legs of 1/16-in. rod held against the inside wall by springs. For velocity measurements the water in the system was always recirculated; this was necessary to maintain the water temperature relatively constant ($\sim$ 1°C. rise/hr.). During the mixing experiments the contaminated water was drained, and fresh water was supplied continuously.

The measuring systems were of two types, one for the velocity field (mean velocity, intensity, and spectrum in the mean flow direction) and the other for the concentration field (mean concentration, intensity, and spectrum of the concentration fluctuation).

A miniature pitot-static tube was used for the mean velocity profile measurements and calibration of the hot-film probe. It was inserted into the test section pipe through a small hole in the wall. A linear constant-temperature hot-film anemometer was used to measure all the characteristics of the velocity field and was an integrated unit including a time averaging mean velocity meter and a long time constant, root-mean-square meter.

For the concentration field measurements a new type of probe was developed which consisted of a pair of ¾ mm. diameter fiber glass lines capable of transmitting light. A gap of 1 mm. was maintained between the two ends of the fiber glass lines, thus dictating the actual volume element that could be probed (5.6×10^{-4} cc.). One of the fiber glass lines was connected to a light source and the other to an optical detecting device. The choice of the light probe for the concentration measurement, based on the absorption law of Beer, restricted the choice of the secondary fluid to a dye. A light bulb operating on 6-v. d.c., was used as a light source in conjunction with gentian violet as a dye indicator. The attenuation of the input light intensity was measured with a 9-stage photomultiplier tube, the output of which was fed into a d.c. electrometer for the mean light level measurement, and into a r.m.s. meter for the fluctuating light intensity measurement. A detailed description of the light probe including limitations, theory, and auxiliary measuring equipment has been presented elsewhere (*14, 15*).

From the standpoint of hydrodynamics one may raise the criticism that the disturbance caused by the probe tip can be very objectionable. Any attempt to use a probe in a flow system will always present this problem because a probe will sense the modified flow rather than the true one. However it would be a very formidable task to examine such a problem carefully; no attempts have so far been made for the case of a hot-wire (or film) probe. One must simply assume that what the probe tip observes will be very close to the representative statistical phenomena actually occurring in the small volume element. However this type of probe is novel in the statistical measurement of concentration, and there is certainly room for constructive criticism and improvement.

For the velocity and concentration spectra measurements wave analyzers were used to separate the various frequency components of the random signal into its respective amplitudes. A power spectral analyzer with analogue squaring and integrating networks to give a spectrum in conjunction with the wave analyzers was used.

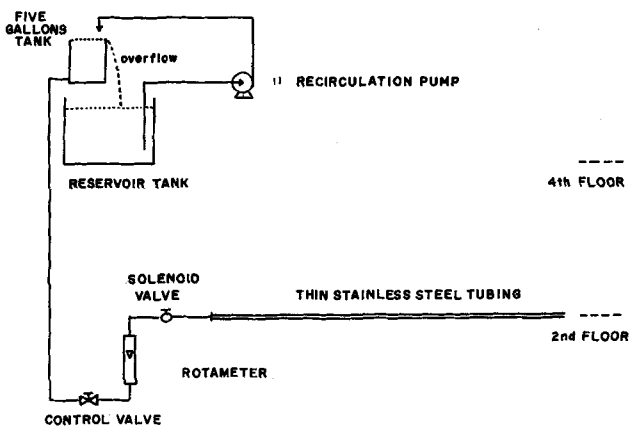

Fig. 2. Layout of injection system.

A mechanical probe mount unit was designed; it consisted of a body frame which was fitted almost tightly inside the test-section pipe and a probe-holding chuck connected to a series of gears. The gears were connected to a driving rod which was extended outside of the test section pipe; thus the probe could be moved in a radial direction by simply turning the gear driving rod externally. The hot-film and fiber optic probes were supported by the probe mount unit and were always stationed at 43 ft. from the upstream end and 5 ft. from the downstream end of the test-section pipe. This distance was dictated by the fiber glass line length of 6 ft. The entrance length of 43 ft. provided a L/d ratio of approximately 170; this can be compared to the ordinary rule of thumb of about 50 for the turbulent entrance length ratio. Even when the injection tube was kept at the maximum separation distance of 10 ft. from the probe, the L/d still remained at 130. The measurements extended to 1.5 in. from the center, which corresponds to a value of R/R_0 of 0 to 0.9764.

EXPERIMENTAL RESULTS

The present experimental work on turbulent mixing involved injecting a dye solution (100 mg./liter of gentian violet at a rate of 0.822 liter/min.) from a single nozzle into water flowing at a Reynolds number of 50,000 based on the maximum mean velocity.

Velocity Measurements

Mean Velocity and Intensity Profiles. To ensure that the turbulent velocity profile at the probe station was fully developed a mean velocity profile was measured with the pitot-static tube and the hot-film probe. The Reynolds number of the flow was the same as Laufer (*13*) used for the study of the turbulent structure in the pipe flow of air. The profile taken at an average temperature of 24°C. and a maximum mean velocity of 1.829 ft./sec. deviated from the corresponding measurements of Laufer by less than 1½%. The consistency of the measured profile was tested by comparing the measured average velocity across the pipe with that computed indirectly from the measured velocity profile. The computed ratio of the average to the maximum mean velocities was 0.816; the actual ratio was 0.809. These agree to within 1%.

The intensity profile in the mean flow direction was measured and is reported as a part of Figure 4; however more extensive and accurate measurements have now been reported by Cohen (*3*). In general the profile shapes are similar to those found by Laufer (*13*) but are somewhat flatter near the center line. The values were about 20% higher on a dimensionless basis and were a weak function of the Reynolds number.

Disturbance. The presence of an injection tube introduces an undesirable disturbance which cannot be avoided completely but which can be minimized. The tube distorts the mean velocity profile only within a short distance from the injection point. The profile can be partially restored by injecting the secondary fluid, even though a complete recovery to the undisturbed profile can never be realized. In order to avoid as much as possible the undesirable mixing at the injection point, the flow rate of the secondary fluid was adjusted to give the best possible restored mean velocity profile across the pipe. An injection velocity of 2.355 ft./sec. was chosen, and the recovery of the mean velocity profiles is shown in Figure 3.* In this figure the maximum mean velocity refers to the undisturbed profile value (1.83 ft./sec.). Actually the integrate volumetric flow should be the same for each curve; however not enough points were obtained to allow an accurate integration. The mean velocity profiles are influenced insignificantly beyond a distance of 2 ft. (8 L/d) in spite of the injection tube.

* The mean velocity profiles surveyed by the pitot-static tube for different injection velocities at separation distances of 1 and 12 in. are available elsewhere (*14*).

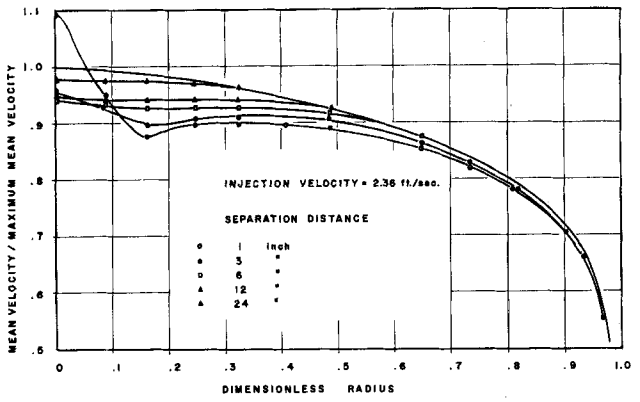

Fig. 3. Mean velocity profile recovery.

The r.m.s. values of the turbulent velocity measured at different separation distances for the chosen injection velocity are shown in Figure 4; these indicate that the effect of the disturbance is strongly reflected in the turbulent velocity intensity. The profile for no disturbance was obtained without the injector in place. A slight increase near the center was observed but was not confirmed by later results (3). It appears to have been associated with the drift experienced with the hot-film anemometer. In any event the effect of the injector is small beyond 2 ft.

Concentration Measurements

The separation distances between the injection point and the light probe were 1, 3, 6, 9, and 12 in. and at 6-in. intervals from there on to a total distance of 90 in.

Mean Concentration Profiles. Since there was one injection source at the center of the pipe, the mean concentration profiles are bell shaped, as would be observed in a jet, and progressively spread towards the wall. Since the pipe wall is impermeable and there exists no internal sink for the dye, the mean concentration profile becomes flatter and gradually approaches the final uniform concentration level dictated by the amount of dye injected and the total water flow. The gradients of the mean concentration profile with respect to the radial coordinate must vanish at the center and wall owing to the symmetry in geometry and impermeability of the wall, respectively. Some typical mean concentration profiles are presented in Figure 5.* Numerical integration for the amount of dye flowing for each profile agreed with the initial injection rate to within 2.5%.

* The complete mean concentration profile figures can be found elsewhere (*14*).

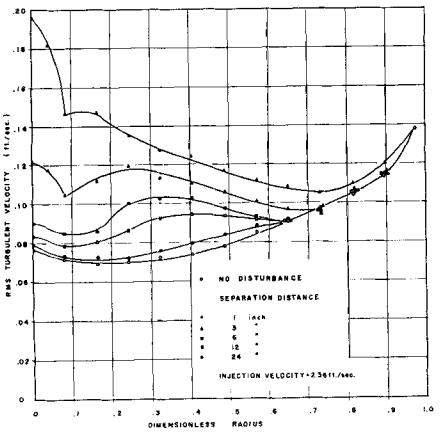

Fig. 4. Root-mean-squared turbulent velocity for various separation distances.

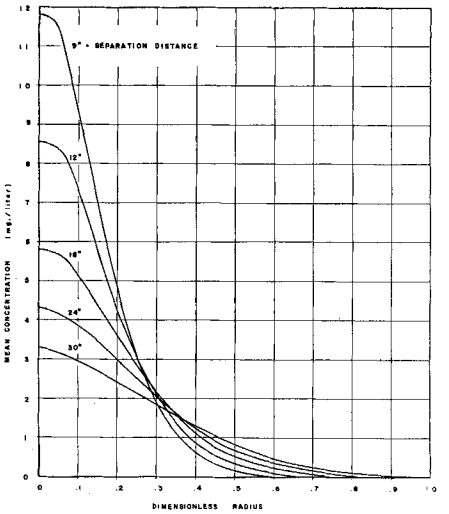

Fig. 5. Mean concentration profile.

Concentration Fluctuation Intensity. Except for the region very close to the injection point, the concentration fluctuation intensity was always higher at the center, decreased monotonically to the wall, and decreased rather rapidly with distance from the injection point. This can be rephrased as the concentration fluctuation intensity persisted longer at the center line than anywhere else in the pipe. This may be a simple consequence of the injection setup, in which much of the injected dye is conveyed along the center line, and of the higher turbulent velocity intensity near the wall contributing to vigorous mixing in this area. The r.m.s. values of the concentration fluctuations at some separation distances are shown in Figure 6.* The ratio of the r.m.s. concentration fluctuations to the mean concentration is also presented elsewhere.* For separation distances up to 42 in. the ratio $c'/\overline{C}$ approaches 100% near the edge of the mean concentration profile; in this case the average of the concentration fluctuations roughly corresponds to the mean concentration itself. It must be noted that at the edge the values for the concentration fluctuation intensity and mean concentration are individually very small.

Intensity of Segregation. The concentration fluctuation intensity persists at the center-line region longer than any-

* Complete rms of concentration fluctuation figures and $c'/\overline{C}$ figure are in reference *14*.

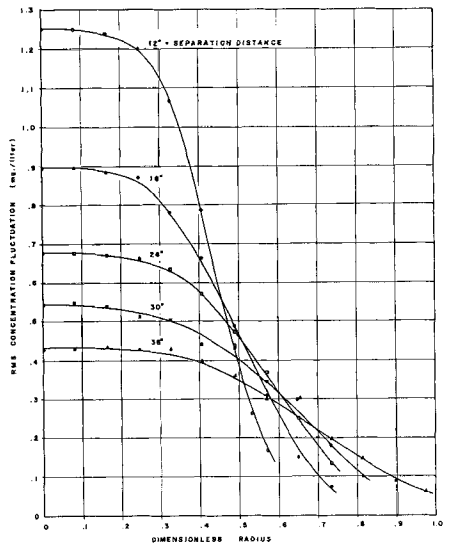

Fig. 6. Root-mean-squared concentration fluctuation profile.

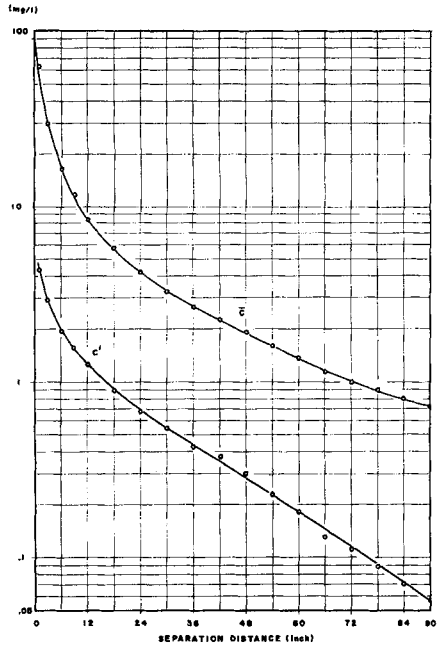

Fig. 7. Mean concentration and decay at the center-line region.

where else. This suggests that if one could define the decay at the center line, the result could serve as an upper limit for the whole region of the pipe. For the center line the decay of the mean concentration and the r.m.s. concentration fluctuations are plotted in Figure 7. The decay of the r.m.s. concentration fluctuations is very rapid, but this is not the true decay because of the superimposed strong decay of the mean concentration as indicated by Figure 7.

In order to circumvent this latter difficulty and in an attempt to recover the true decay of the concentration fluctuation intensity, the intensity of segregation first defined by Danckwerts (9) can be used:

$$I_s = \overline{m^2}/\overline{M}\,\overline{N} \qquad (9)$$

where $\overline{m^2} = \overline{(M - \overline{M})^2}$. The reason for the choice of Equation (9) is that I_s has the value of 1 when M and N are unmixed (completely segregated) and the value of 0 when the mixing is completed (uniform concentration). I_s has the same representation as the normalized concentration fluctuation intensity obtained from the solution for the decay in isotropic turbulent mixing. A complete equivalence exists for the case of an isotropic field in which there is no mean concentration. In addition to providing the true intensity, independent of the decay of mean concentration, the representation in terms of the intensity of segregation has the advantage that it takes account of the volume ratio between the two components. The data at the center line are expressed in terms of the intensity of segregation (adjusted so that $I_s = 1$ at zero separation) and are plotted in Figure 8. This is taken as the true decay of concentration fluctuation intensity in the absence of superimposed mean concentration decay.

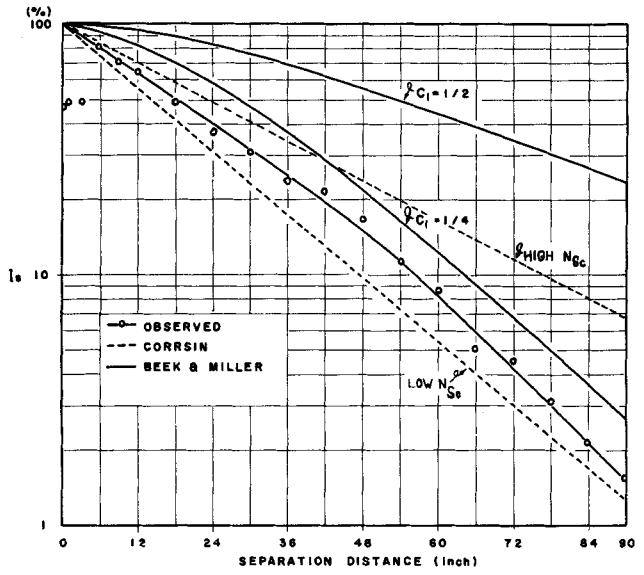

Fig. 8. Intensity of segregation.

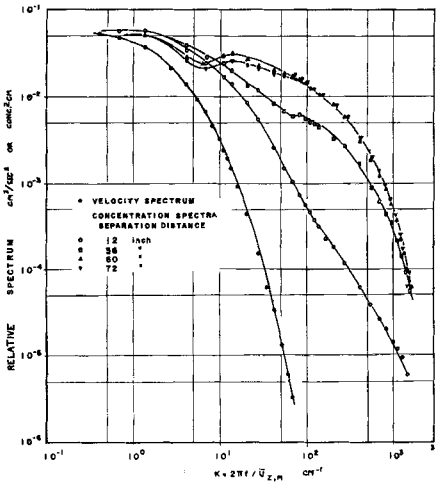

Fig. 9. Relative spectra.

Spectra. All spectra measurements (Figure 9) were made at the center line. For conversion to wave numbers the Taylor space-time interchange was assumed valid, since the mean velocity is quite constant in the center-line area and since the turbulent intensity was relatively low (4%). No further corrections are reported here; however before quantitative use of the concentration spectra can be made some attempt to correct for the finite size of the probe would be necessary. No corrections are necessary for the velocity spectrum which was used in the later calculations. All spectra are presented in Figure 9 on an arbitrary relative scale for better comparison; the concentration spectra would otherwise decay in accordance with the concentration fluctuation intensity as given in Figure 7.

DISCUSSION

At present it is not feasible to develop a theory which describes the decay of intensity in the whole region of a pipe; this would be the problem of a nonisotropic, inhomogeneous scalar field in a turbulent shear flow. The theory even for the idealized case of isotropic velocity and concentration fields cannot be considered as satisfactorily resolved; thus the question being posed involves formidable difficulties as fully discussed elsewhere (*14*).

Phenomenological Approach

One possible approach is the use of the eddy diffusivity concept. Consequently values of $\overline{u_r c}$ were obtained from the mean velocity and concentration profiles for various separation distances (*14*). From these values of ϵ_s were obtained. The eddy diffusivity and viscosity were expressed in terms of the more conventional ratio $\alpha_T = \epsilon_s/\epsilon$, a reciprocal turbulent Schmidt number. The result indicates that α_T is around 0.8 for separation distances up to 24 in. but increases rapidly to almost 160 at a separation distance of 84 in. This is mainly because ϵ is unchanged along the distance, but the gradient of the mean

concentration profile becomes very small downstream making the eddy diffusivity $\epsilon_s = -\overline{u_r c}/(\partial \overline{C}/\partial R)$ very large. The usefulness of this sort of approach generally relies on the observation that the ratio α_T can be treated as a slowly varying function of the flow characteristics and geometry, if not practically a constant. However in this case such a wide variation seems to defy the utility of this phenomenological approach.

Decay at the Center Line

A more fruitful approach was to compare the results for the decay at the center line with the predictions from isotropic theory. By this it is not meant to imply that the flow at the center was isotropic, but rather that isotropic theory may provide a crude estimate to the mixing at the center line even though the flow is of a shear type. If the prediction is reasonable, it can be used to estimate the required mixing time, since the center line was the last area to be mixed for the geometry selected. This would constitute a use of isotropic theory, not a proof. There is some hope of success, since it is the center-line area in pipe flow that is closer to isotropic conditions than any other location. Although the spectrum to be discussed indicated a lack of isotropic conditions in detail, Cohen (3) did find an equality of the three components of the r.m.s. velocities at the center line in the same apparatus.

In the analysis to follow isotropy will be assumed, so that comparison to the pipe shear flow data can be made. First consider the equation for the decay of normalized intensity for the low Schmidt number case obtained by Corrsin [see Equations (3) and (4)]; that is

$$\ln [\overline{c^2(t)}/\overline{c^2(0)}] = -t/\tau = -6\nu t/\lambda_g^2 \qquad (10)$$

λ_g can be obtained directly from the spectrum measurements as follows. The relative spectrum is uniformly adjusted so that the relation

$$u_z'^2 = \int_0^\infty \phi(k)\, dk \qquad (11)$$

is satisfied. The velocity energy dissipation can then be determined from

$$\epsilon = 15\,\nu \int_0^\infty k^2\, \phi(k)\, dk \qquad (12)$$

and λ_g in turn from

$$\lambda_g^2 = 15\,\nu u_z'^2/\epsilon \qquad (13)$$

For the specific case under consideration the mean-velocity-squared was 5.406 sq. cm./sec.^{2}, and the calculated energy dissipation was 14.9 sq. cm./sec.^{3}. For a kinematic viscosity of 0.01 sq cm./sec., Equation (13) and the above values give 0.233 cm. for the microscale. The actual elapse time in Equation (10) can be replaced by the length traveled by a blob of fluid moving at the central maximum mean velocity $\overline{U}_{z,m}$; that is

$$t \cong L/\overline{U}_{z,m} \qquad (14)$$

The maximum mean velocity was 55.7 cm./sec., and with this the right side of Equation (10) becomes $-t/0.91 = -0.604\,L$, where t is in seconds and L is in feet. The curve for this low Schmidt number case, with a time constant of 0.91 sec., is shown in Figure 8. It falls below the data.

The low Schmidt number case can be extended to the high Schmidt range, since the scalar macroscale should depend on the manner of injection and not upon the Schmidt number level. Thus the time constant already obtained can be used in Equation (5) to estimate the term $(L_s^2/\epsilon)^{1/3}$, which in turn can be used in Equation (6) to obtain time constant for the high Schmidt number case. The Schmidt number is 7,760, corresponding to a molecular diffusivity of 1.288×10^{-6} sq. cm./sec. (23). All other terms are known, and the new time constant becomes 1.48 sec. The coefficient for the decay in terms of feet drops from 0.604 to 0.37, which is also shown in Figure 8. Corrsin's analysis is not an exact solution to the isotropic mixing problem and is even more approximate for the shear flow; thus the coefficients are not expected to be exactly correct. The test of the equations offered here is very stringent in that ratios of low to high Schmidt number experiments are not used so that the absolute values of the constants would fall out. Thus one must consider the curves, which bracket the experimental points, to be very good estimates of mixing.* Further analysis of the contribution of the various terms in Equation (6) shows that the correction is somewhat over 60% between the low and high Schmidt number cases; however the term that actually contains the Schmidt number contributes about 13% of this. At the high Schmidt number range a change of a factor of 10 in this number ($\sim$ 700 for salt in water to $\sim$ 7,000 for the dye) causes only a little over a 3% change in the time constant.

For general use in mixing calculations the estimation of the microscale from the velocity spectrum is not desirable, since this measurement may not be always available. Thus the following alternate semiempirical method is suggested. The microscale can be approximated by the empirical relation

$$\lambda_g^2 = 10\,\nu\, L_f/C_2 u_z' \qquad (15)$$

where C_2 is a numerical constant of about 1.1. When one follows the suggestion made by Hinze (*10*), the macroscale L_f can be approximated by

$$L_f \cong (3/4)\,(1/k_o) \qquad (16)$$

Unlike the small eddies the average size of the energy containing eddies $1/k_o$ is influenced by the linear dimension of the pipe from which it received the energy directly. The following relation can then be written on a dimensional basis

$$1/k_o = C_1 R_o \qquad (17)$$

where C_1 is dimensionless and which Beek and Miller (2) suggested as having a value of ½. Combining Equations (15) through (17) into Equation (5) one gets an estimate of the time constant for the low Schmidt case

$$\lambda_g^2/6\nu \cong 10\,C_1\,R_o/8\,C_2\,u_z' \cong 0.568\,R_o/u_z' \qquad (18)$$

which gives a final value of 0.95 sec. This is a very good estimate for the value of 0.91 obtained from the spectrum calculation.

The results of Beek and Miller can also be compared with the experimental points. To do this the dimensionless time used in their figures must be expressed in terms of L with the aid of Equations (14) and (16); that is

$$\sigma = k_o\, u_z'\, t = (1/C_1 R_o)\,(u_z'/\overline{U}_{z,m})\, L \qquad (19)$$

or

$$L = 2.99\, C_1\, \sigma \qquad (20)$$

Their curve was estimated for a value of C_1 of ½ and is plotted in Figure 8. The estimation is not for exactly the same conditions, and one would expect any change to give even poorer agreement; however the actual shape of the decay curve is closer to that observed than the straight line of Equation (10). A value of C_1 of ¼ gives a better estimation.

It is clear that the decay of normalized concentration fluctuation intensity roughly follows the predicted exponential law, and the scalar contaminant has decayed to

* Professor Corrsin has informed the author that slight modification is necessary for Equations (4) and (5). A preliminary calculation indicated a considerable improvement in the comparison, which will be reported in a note at a later date. It might be well to emphasize that the use of these equations does not involve arbitrary constants.

nearly 99% of the initial value at 90 in. downstream from the injection point. In retrospect, for the prediction of the decay of concentration fluctuation intensity, the results of Corrsin (with $C_1 = \frac{1}{2}$) and of Beek and Miller (with $C_1 = \frac{1}{4}$ rather than $\frac{1}{2}$) seem to provide the necessary information and can be considered useful for practical problems.

Spectra

The velocity spectrum (Figure 9) does not exhibit a $-5/3$ power wave number range as predicted from local isotropic turbulent theory, which shows that true isotropy did not exist at the center line. The concentration spectra at 1 and 3 ft. differ not only from each other but also from those taken at 5 and 6 ft. At 1 ft. the spectrum drops with $-5/3$ power for high k, which can be interpreted to mean a simple scalar spectral energy cascade. The appearance of the $-5/3$ power wave number range should not be associated with the consequence of local isotropy in the concentration field. Owing to the huge difference in ν and D in water, the spectrum of concentration fluctuations extends much farther to the higher wave number range than that of velocity fluctuation; therefore the dissipation subrange of the velocity spectrum corresponds roughly to the convective subrange of the concentration spectrum and thus enhances the cascade process of the breaking up of the larger to smaller eddies.

On the other hand, owing to the small D, the smaller eddies cannot be diffused as fast as they are supplied from the convective subrange. Therefore a state of imbalance results between the supply of small eddies from the convective subrange and diffusional dissipation of small eddies to the higher k range. This was clearly demonstrated by the spectra at 3, 5, and 6 ft., which have not only a flattened spectrum for the convective subrange and a steeper spectrum for the dissipation subrange but also show a small hump. The location of the hump on the concentration spectra shifts gradually to the smaller k as the separation distance increases. This is not in accord with the theoretical predictions of Beek and Miller; furthermore the imbalance in the form of a hump appears to be less dramatic than suggested by their computation. Nevertheless the theory predicts the hump and in approximately the correct position.

ACKNOWLEDGMENT

The authors wish to acknowledge the financial assistance of the National Science Foundation (Grant G-9400) which made this work possible. The Ohio State University provided the initial support for the work by both a graduate assistantship (JL) and by the purchase of some of the key equipment.

NOTATION

C_1, C_2 = constants defined in the text
c = fluctuating concentration
d = pipe diameter
D = molecular diffusivity
$E(k,t), E_s(k,t)$ = velocity and scalar quantity energy spectrums
f = frequency, cycles per sec.
I_s = intensity of segregation [Equation (9)]
k = wave number
k_o = wave number associated with energy containing velocity eddies
L = pipe length
L_f, L_s = velocity and scalar macroscale
$M, \overline{M}$ = total and mean concentrations in volume fraction of component M
$N, \overline{N}$ = total and mean concentration in volume fraction of component N
N_{Sc} = Schmidt number $= \nu/D$
R_o = pipe radius
R, Z, θ = polar cylindrical coordinates
$S, \overline{S}, s$ = total, mean, and fluctuating scalar quantities
t = time
$U_i, \overline{U}_i, u_i$ = total, mean fluctuating ith velocity components
u_i' = root-mean-squared velocity of the ith component
$\overline{U}_z$ = $\overline{U}$ in Z axis
α_T = ϵ_s/ϵ

Greek Letters

ϵ = velocity energy dissipation per unit mass
ϵ, ϵ_s = eddy viscosity and diffusivity in physical space
$\epsilon_s(k)$ = eddy diffusivity in wave number space [Equation (8)]
$\lambda_s, \lambda_f, \lambda_g$ = microscales
ν = kinematic viscosity
τ = time constant
σ = $k_o u_z' t$
π = 3.1416 . . .
$\phi(k)$ = one-dimensional scalar spectrum

Subscripts

m = maximum value
= root-mean-square
overscore = average

LITERATURE CITED

1. Batchelor, G. K., *J. Fluid Mech.*, **5**, 113 (1959).
2. Beek, J., Jr., and R. S. Miller, *Chem. Eng. Progr. Symposium Ser. No. 25*, **55**, 23 (1959), and private communication.
3. Cohen, M. F., M.S. thesis, The Ohio State University, Columbus, Ohio (1962).
4. Corrsin, S., *J. Appl. Phys.*, **22**, 469 (1951).
5. ———, *J. Aeronaut. Sci.*, **18**, 417 (1951).
6. ———, "Proceedings of the First Iowa Thermodynamics Symposium," Iowa State Univ. (1953).
7. ———, *A.I.Ch.E. Journal*, **3**, 329 (1957).
8. ———, Paper presented at the A.I.Ch.E. annual meeting, Chicago, Ill. (Dec., 1962).
9. Danckwerts, P. V., *Appl. Sci. Res.*, **A3**, 279 (1953).
10. Hinze, J. O., "Turbulence," McGraw-Hill, New York (1959).
11. Kistler, A. L., V. O'Brien, and S. Corrsin, *Natl. Advisory Comm. Aeronaut. RM 54D19* (1954).
12. Lamb, D. E., F. S. Manning, and R. H. Wilhelm *A.I.Ch.E. Journal*, **6**, 682 (1960).
13. Laufer, J., *Natl. Advisory Comm. Aeronaut. Rept. 1174* (1954).
14. Lee, Jon, Ph.D. thesis, The Ohio State University, Columbus, Ohio. Available from University Microfilms, Ann Arbor, Michigan, request Mic. 63-63, Xerox, $13.05, microfilm, $3.70 (1962).
15. ———, and Robert S. Brodkey, *Rev. Sci. Inst.*, **34**, 1086 (1963).
16. Manning, F. S., and R. H. Wilhelm, *A.I.Ch.E. Journal*, **9**, 12 (1963).
17. Mills, R. R., Jr., A. L. Kistler, V. O'Brien, and S. Corrsin, *Natl. Advisory Comm. Aeronaut. Tech. Note 4288* (1958).
18. O'Brien, E. E., and C. C. Francis, *J. Fluid Mech.*, **13**, 369 (1962).
19. Obukhov, A. M., *Izv. Akad. Nauk. USSR, Ser. Geogr. i Geofiz.*, **13**, 58 (1949).
20. Prausnitz, J. M., and R. H. Wilhelm, *Rev. Sci. Instr.*, **27**, 941 (1956).
21. ————————, *Ind. Eng. Chem.*, **49**, 978 (1957).
22. Rosensweig, R. E., H. C. Hottel, and G. C. Williams, *Chem. Eng. Sci.*, **15**, 111 (1961); and Ph.D. thesis, Mass. Inst. Technol., Cambridge, Massachusetts (1959).
23. Wilke, C. R., *A.I.Ch.E. Journal*, **1**, 264 (1955).

Manuscript received November 26, 1962; revision received August 26, 1963; paper accepted August 29, 1963. Paper presented at A.I.Ch.E. Chicago meeting.